An Asparagine-Phenylalanine Substitution Accounts for Catalytic Differences between hGSTM3-3 and Other Human Class Mu Glutathione *S*-Transferases[†,‡]

Yury V. Patskovsky, Larysa N. Patskovska, and Irving Listowsky*

Department of Biochemistry, Albert Einstein College of Medicine, Bronx, New York 10461

Received July 26, 1999; Revised Manuscript Received September 28, 1999

ABSTRACT: The hGSTM3 subunit, which is preferentially expressed in germ-line cells, has the greatest sequence divergence among the human mu class glutathione *S*-transferases. To determine a structural basis for the catalytic differences between hGSTM3-3 and other mu class enzymes, chimeric proteins were designed by modular interchange of the divergent C-terminal domains of hGSTM3 and hGSTM5 subunits. Replacement of 24 residues of the C-terminal segment of either subunit produced chimeric enzymes with catalytic properties that reflected those of the wild-type enzyme from which the C-terminus had been derived. Deletion of the tripeptide C-terminal extension found only in the hGSTM3 subunit had no effect on catalysis. The crystal structure determined for a ligand-free hGSTM3 subunit indicates that an Asn212 residue of the C-terminal domain is near a hydrophobic cluster of side chains formed in part by Ile13, Leu16, Leu114, Ile115, Tyr119, Ile211, and Trp218. Accordingly, a series of point mutations were introduced into the hGSTM3 subunit, and it was indeed determined that a Y119F mutation considerably enhanced the turnover rate of the enzyme for nucleophilic aromatic substitution reactions. A more striking effect was observed for a double mutant (Y119F/N212F) which had a k_{cat}/K_m^{CDNB} value of 7.6×10^5 s^{-1} M^{-1} as compared to 4.9×10^3 s^{-1} M^{-1} for the wild-type hGSTM3-3 enzyme. The presence of a polar Asn212 in place of a Phe residue found in the cognate position of other mu class glutathione *S*-transferases, therefore, has a marked influence on catalysis by hGSTM3-3.

Glutathione *S*-transferases (GSTs)[1] probably protect cells against toxic insults from electrophilic compounds by catalyzing nucleophilic addition or substitution reactions between GSH and those types of reactive substances (*1*−*10*). Although GSTs are highly selective for GSH as the nucleophile, they are notably nonspecific with regard to the types of electrophilic second substrates that they can detoxify or modify (*11*−*16*). These cytosolic enzymes are characterized by two-domain structures in which structurally conserved GSH binding sites (G-sites) are largely made up through interactions with residues of the N-terminal domain, and binding of the second substrates (H-sites) involves residues of the C-terminal part and other segments of the protein (*17*−*25*). GSTs are also known to bind many different types of nonsubstrate ligands (*6*, *26*−*28*). Mammalian GSTs are products of gene superfamilies (*29*−*32*), and a species-independent nomenclature system has been devised for assigning the major forms into alpha, mu, pi, and theta classes on the basis of sequence homologies, dimeric subunit assembly patterns, and other common properties (*33*, *34*).

Within each individual class of GSTs, differences in substrate specificity may be attributed to a limited number of amino acid substitutions at their H-sites. Multiple variants of the enzyme thereby broaden the scope of potential substrates that are modified and thereby detoxified. A common chemical step of GST catalysis involves activation of the enzyme-bound GSH by lowering the pK_a of its thiol group (*13*, *16*, *35*−*38*). Of the cluster of human mu class GST genes on chromosome 1, four (*hGSTM1*, *hGSTM2*, *hGSTM4*, and *hGSTM5*)[2] are closely related and probably originated from gene conversion or duplication events (*39*−*41*). The single *hGSTM3* gene is most distantly related to the others (*42*−*44*). The hGSTM3 subunit is also structurally distinct from the other human mu class GSTs with only about 70% amino acid sequence identity and four-residue N-terminal and three-residue C-terminal extensions (*42*). There are also rodent counterparts of hGSTM3 (*45*), and these represent a unique subgroup of the class mu enzymes that are primarily expressed in postmeiotic germ-line cells of testis; they are, by far, the preponderant GST forms in mature spermatozoa (*46*), but are present at very low levels in most somatic cells (*47*).

Most cytosolic GSTs catalyze nucleophilic aromatic substitution reactions with different substrates, including the commonly used 1-chloro-2,4-dinitrobenzene (CDNB), but the hGSTM3-3 enzyme is less effective than other mu class enzymes in catalyzing these types of reactions (*45*). The hGSTM5 subunit is another mu class GST that is expressed

[†] This work was supported by Grant CA 42448 from the National Cancer Institute.

[‡] The coordinates for the structure of the recombinant hGSTM2-3 enzyme have been deposited in the Brookhaven Protein Data Bank under file name 3GTU.

* To whom correspondence should be addressed. Telephone: (718) 430-2276. Fax: (718) 430-8565. E-mail: irving@aecom.yu.edu.

[1] Abbreviations: GST, glutathione *S*-transferase; GSH, glutathione; CDNB, 1-chloro-2,4-dinitrobenzene; CDNBA, 1-chloro-3,5-dinitrobenzoic acid; RT-PCR, reverse transcriptase-polymerase chain reaction; rsmd, root-mean-square deviation.

[2] For nomenclature of GSTs, see ref *34*.

10.1021/bi991714t CCC: $18.00
Published on Web 11/11/1999

Table 1: Oligonucleotides Used for Engineering of Recombinant Wild-Type and Mutant Human Mu Class GSTs

primer	position[a]	sequence[b]
M3-sense	−11 → 19	5′-AGC CCG TCC ATA TGT CGT GCG AGT CGT CTA-3′
M5-sense	−9 → 18	5′-ACC AGC CAT ATG CCC ATG ACT CTG GGG-3′
M3-reverse	696 → 667	5′-TGC AAG TCT GGA TCC TGA TCA GCA TAC AGG-3′
M5-reverse	696 → 671	5′-GGT TGG ATC CTC CCT CCC ATC TTC TG-3′
M3A198S-sense	571 → 603	5′-CGT TTT GAA GCT TTG GAG AAG ATC TCT GCC TAC-3′
M3A198S-reverse	603 → 571	5′-GTA GGC AGA GAT CTT CTC CAA AGC TTC AAA ACG-3′
M3(N212G)	669 → 631	5′-AGG CTT GTT GCC CCA CTG GGC CAT CTT GTT *GCC* GAT GGG-3′
M3(N213G)	669 → 631	5′-AGG CTT GTT GCC CCA CTG GGC CAT CTT *GCC* GTT GAT GGG-3′
M3(N212F)	669 → 631	5′-AGG CTT GTT GCC CCA CTG GGC CAT CTT GTT *GAA* GAT GGG-3′
M3(N212G/N213G)	669 → 631	5′-AGG CTT GTT GCC CCA CTG GGC CAT CTT *GCC GCC* GAT GGG-3′
M3(N212F/N213G)	669 → 631	5′-AGG CTT GTT GCC CCA CTG GGC CAT CTT *GCC GAA* GAT GGG-3′
M3-common	687 → 652	5′-GCC GGA TCC TCA GCA TAC AGG ATT GTT GCC CCA CTG-3′
M3(delPVC)-reverse	684 → 655	5′-TCC TGA TCA GGA TCC *TCA* CTT GTT GCC CCA-3′
M3(Y119F)-reverse	372 → 349	5′-TGG TCA GAG CTG *AAA* CAG AGC CT-3′
M3(Y119F)-sense	349 → 372	5′-AGG CTC TGT *TTC* AGC TCT GAC CA-3′
M3(Y119A)-reverse	372 → 349	5′-TGG TCA GAG CT*G GC*A CAG AGC CT-3′
M3(Y119A)-sense	349 → 372	5′-AGG CTC TGT *GCC* AGC TCT GAC CA-3′

[a] The first and last bases of primers are shown as the distances from the first A (+1) of ATG encoding the initiating Met residue. [b] Restriction sites are underlined, and mutated codons are italicized.

at very low levels in most human tissues (*43*, *47*); therefore, a catalytically active hGSTM5-5 enzyme has not yet been characterized. In this study, the crystal structure of the hGSTM3 subunit was determined. Chimeric enzymes were engineered by modular interchange of the divergent C-terminal domains and by incorporation of point mutations at certain positions in the hGSTM3 and hGSTM5 subunits. The results indicate that the characteristic catalytic properties of hGTM3-3 are, to a great extent, determined by the presence of an Asn212 residue in place of phenylalanine found at the cognate position in other mu class enzymes.

MATERIALS AND METHODS

Materials. 1-Chloro-2,4-dinitrobenzene (CDNB) and 4-chloro-3,5-dinitrobenzoic acid (CDNBA) were obtained from Aldrich Chemical Co. (St. Louis, MO). Reduced glutathione and GSH−agarose were obtained from Sigma Chemical Co. (St. Louis, MO).

Expression of Recombinant Homodimeric hGSTM3-3 and hGSTM5-5 Enzymes. Oligonucleotides described in this report were obtained from Perkin-Elmer Inc. (Perkin-Elmer Cetus, Emeryville, CA). The cDNAs for hGSTM3-3 and hGSTM5-5 were amplified using RT-PCR (reverse transcriptase-polymerase chain reaction) with sets of sense and antisense specific primers listed in Table 1. Total RNA was purified from HeLa or HepG2 human cell lines using a QIAGEN purification kit (QIAGEN Inc., Chatworth, CA) according to the manufacturer's instructions. The reverse oligonucleotides served as primers for reverse transcriptase *RAV-2* (Amersham Life Science Inc., Cleveland, OH), and synthetic cDNAs were added as templates for the PCR procedures. Resultant PCR fragments were subcloned into the pET3a expression vector, as described in a previous report (*45*). Recombinant plasmid DNAs were then purified and sequences determined using an ABI 377 Applied Biosystems automated sequencer (Perkin-Elmer Inc.), utilizing T7-promoter and T7-terminator primers. The fidelity of DNA sequencing procedures was confirmed by electrospray ionization mass spectrometry (ESI-MS) of the recombinant proteins that were produced, using an API-III triple-quadrupole mass spectrometer (PE-SCIEX) as described by Rowe et al. (*47*). The molecular masses measured for recombinant wild-type GST protein subunits (hGSTM3, 26428 ± 2 Da; and hGSTM5, 25544 ± 2 Da) corresponded to those deduced from the cDNA nucleotide sequences.

Construction of hGSTM3-3 Mutant GSTs and the hGSTM3−hGSTM5 Chimera. Each cDNA encoding a mu class GST (except for the cDNA of the GSTM3 subunit) contains a unique restriction site for a *Bgl*II at position 579, thus dividing the coding region into two unequal segments. The smaller segment carries the part of the coding region for amino acid residues 194−217 (C-terminus). A corresponding site for *Bgl*II was introduced into the appropriate region of the cDNA for GSTM3 by genetic engineering methods (with an additional A198S substitution; see Table 1). To construct modular chimeric enzymes, the *Bgl*II−*Bam*HI cDNA fragments encoding C-termini of distinct GST subunits were ligated with *Nde*I−*Bgl*II cDNA fragments encoding the N-termini, and subcloned into the pET3a vector.

Residues Tyr119, Asn212, and Asn213 of hGSTM3 [corresponding to residues Tyr115, Phe208, and Gly209 of hGSTM5 (see Figure 1A)] were mutated by PCR methods with an appropriate set of oligonucleotides (Table 1). The hGSTM3-3 mutants were constructed with one, two, or three point mutations. These were Tyr119Ala, Tyr119Phe, Asn212Gly, Asn213Gly, and Asn212Phe single mutants, Asn212Gly/Asn213Gly, Asn212Phe/Asn213Gly, Tyr119Ala/Asn212Phe, and Tyr119Phe/Asn212Phe double mutants, and Tyr119Ala/Asn212Phe/Asn213Gly and Tyr119Phe/Asn212Phe/Asn213Gly triple mutants. The amplified DNA fragments were purified and cloned into the pET3a vector, and sequences were determined as described above.

Purification of Recombinant Enzymes and Assays of Enzyme Activity. The recombinant wild-type and mutant enzymes were purified by GSH affinity chromatography as described previously (*47*) and dialyzed extensively against buffer containing 20 mM Tris-HCl (pH 7.5), 1.0 mM DTT, and 0.2 mM EDTA, particularly to prevent oxidation of hGSTM3-3 and its mutant counterparts.

Stopped-flow spectrophotometric measurements were performed as previously described (*49*). The concentrations of reactants were varied (from 100 to 1000 μM for GSH and from 50 to 1000 μM for CDNB). The final protein concentration was adjusted to 10 or 20 μM, to ensure that

A

```
                10        20        30        40        50
hGSTM5      MPMTLGYWDIRGLAHAIRLLLEYTDSSYVEKKYTLGDAPDYDRSQWLNEKFKLGLDFPNL
hGSTM3   MSCESS-V-----------------F--T--E--R--C-E----------DV----D------

            60        70        80        90        100       110
hGSTM5      PYLIDGAHKITQSNAILRYIARKHNLCGETEEEKIRVDILENQVMDNHMELVRLCYDPDF
hGSTM3      ---L--KN-----------------M-------------I------FRTQ-I----SS-H

            120       130       140       150       160       170
hGSTM5      EKLKPKYLEELPEKLKLYSEFLGKRPWFAGDKITFVDFLAYDVLDMKRIFEPKCLDAFLN
hGSTM3      -----Q------GQ--QF-M----FS----E-L------T--I--QN---D-----E-P-

            180       190       200       210
hGSTM5      LKDFISRFEGLKKISAYMKSSQFLRGLLFGKSATWNSK
hGSTM3      --A-MC---A-E--A--LQ-D--CKMPINN-M-Q-GN-PVC
```

B

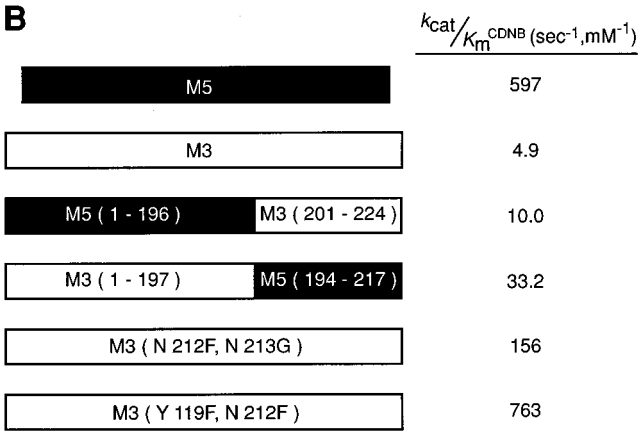

FIGURE 1: (A) Amino acid sequence alignment of hGSTM3 and hGSTM5 subunits. Residues that are identical to those of hGSTM5 are represented by dashes. (B) Schematic representation of recombinant hGSTM3 and hGSTM5 enzymes, and modular chimeric and point mutations of each subunit. The shaded areas represent sequences of the hGSTM5 subunit, and the white areas are those of hGSTM3. Steady-state kinetic data for each representative homodimeric enzyme were obtained with the CDNB substrate as indicated in Materials and Methods.

any initial burst increase of absorbance could be readily detected.

Kinetic parameters with CDNB and GSH as substrates were determined by steady-state kinetic analyses (*48*). The limiting values of rate constants were determined from plots of log k_{cat} or log k_{cat}/K_m^{CDNB} versus pH. Specific activities with 1.0 mM CDNBA and 1.0 mM GSH substrates were measured spectrophotometrically in 0.1 M sodium phosphate (pH 6.2), using the molar extinction coefficients and experimental conditions described previously (*49*).

Modeling of the hGSTM3-3 Catalytic Active Site. The crystal structure of the hGSTM3 subunit was determined and refined to 2.8 Å resolution as a ligand-free heterodimeric hGSTM2-3 enzyme [for structural details, refer to PDB file 3GTU (Y. V. Patskovsky et al., manuscript in preparation)]. The coordinates of hGSTM3 (3GTU) as well as of ligand-free hGSTM2-2 [PDB file 2GTU (*50*)], ligand-free hGSTM1a-1a [PDB file 1GTU (*49*)], and hGSTM2-2(W214F) with GSH bound [PDB file 1HNA (*51*)] were used for modeling of the hGSTM3 catalytic site structure using the INSIGHT II97 program package (Biosym Technologies Inc.). Three-dimensional structures were aligned according to structural homologies of their GSH-binding sites. Overall rmsd values calculated between Cα atoms of these proteins varied over the range of 0.6−0.9 Å, but rmsd values between Cα atoms of residues involved in the formation of G-site structures were about 0.3 Å. Also, there was no significant structural difference between ligand-free hGSTM3 and a GSH-complexed hGSTM2(W214F) G-site structure, so the rmsd value between side chain atoms of these G-sites was only about 0.4 Å. It is evident that G-sites of the mu class GSTs are the most structurally rigid, and evolutionarily conserved domains of these enzymes. It was thus possible to fill the G-site of hGSTM3 with GSH after alignment of the three-dimensional structures of each subunit of hGSTM2-3 and hGSTM2-2(W214F) containing bound GSH, without changing the relative atomic coordinates of neighboring amino acid residues.

RESULTS

Catalytic Properties of Wild-Type, Chimeric, and Mutant Enzymes. Human hGSTM5-5 is a far more active enzyme for conjugating CDNB than is hGSTM3-3 (Table 2). Because of the low abundance of hGSTM5 subunits in most human tissues (*47*), its enzymatic properties have not been examined until now. There is 72% amino acid sequence identity between these two GST subunit types (Figure 1A); some sequence differences are dispersed throughout the polypeptide chain, but most are close to their C-termini, regions with only 43% sequence identity [the antiserum raised against a C-terminal peptide of one subunit does not recognize the other (*43*, *47*)]. The C-terminal 24-residue peptides were therefore subjected to reciprocal modular interchange between hGSTM3 and hGSTM5 subunits, and two novel chimeric enzymes hGST($M3_{1-197}M5_{194-217}$) and hGST-($M5_{1-196}M3_{201-224}$) were engineered (Figure 1B). Despite the pronounced sequence differences between the C-termini, the hGSTM3−M5 chimeric enzymes retained activities with CDNB and CDNBA as substrates (Figure 1B and Tables 2 and 3). Significantly, however, the chimeric enzyme hGST($M3_{1-197}M5_{194-217}$) had a greater catalytic efficiency than the wild-type hGSTM3-3, whereas the chimera $hGST_2(M5_{1-196}M3_{201-224})_2$ was much less active than wild-type hGSTM5-5. Deletion of the extended C-terminal peptide found only in hGSTM3 (Pro-Val-Cys, Figure 1A) did not cause a change in the catalytic properties of the resultant mutant protein (Table 2), but increased the stability of the enzyme and its resistance to oxidation (data not shown). In the crystal structure of the hGSTM3 subunit, this C-terminal tripeptide is directed outward from the protein globule so that the C-terminal Cys residue is exposed to solvent and is distant from the active site pocket.

Comparisons of kinetic parameters of the modular M3−M5 enzymes indicate that some residues of their C-terminal peptides account for the catalytic differences between hGSTM3-3 and hGSTM5-5 (Figure 1B and Table 2). Sequence alignments show that Phe208 (corresponding to Asn2l2 of hGSTM3) is conserved in most human and rodent enzymes that are active with CDNB as a substrate (*6*). Amino acid residue 209 (Asn213 of hGSTM3) is less conserved than Phe208, but is also close to the active site in three-dimensional structures determined for mu class GSTs (*20*−*22*). The corresponding residues of hGSTM5-5 (Phe208 and Gly209) were therefore introduced in place of Asn212 and Asn213 of hGSTM3-3 individually, or together (Figure 1B). The double mutant hGSTM3-3(N212F/N213G) was much more active than hGSTM3-3 (Table 2), with approximately 15-fold greater k_{cat} and 35-fold greater k_{cat}/K_m^{CDNB} values compared to those of wild-type hGSTM3-3. A single point mutation of hGSTM3-3(N212F) yielded greater k_{cat} values

Table 2: Limiting Values of Kinetic Parameters of Recombinant Wild-Type, Chimeric, and Mutant Mu Class GSTs with the CDNB Substrate[a]

protein	K_m^{CDNB} (mM)	K_m^{GSH} (mM)	k_{cat} (s^{-1})	k_{cat}/K_m^{CDNB} (s^{-1} mM^{-1})	k_{cat}/K_m^{GSH} (s^{-1} mM^{-1})
M3-3	1.10	0.084	5.43	4.9	64.6
M3-3(delPVC)	1.0	0.10	4.2	4.2	42.0
M5-5	0.10	0.39	59.7	597.0	153.1
$M3_{1-197}M5_{194-217}$	0.50	0.13	16.6	33.2	127.7
$M5_{1-196}$ $M3_{201-224}$	0.62	0.40	6.2	10.0	15.5
M3(N212F/N213G)	0.48	0.105	75.0	156.2	714.0
M3(N212G/N213G)	0.44	0.11	14.7	33.4	133.6
M3(N212F)	1.20	0.020	27.6	24.2	1380.0
M3(N212G)	0.40	0.10	5.5	13.8	55.0
M3(N213G)	0.41	0.12	14.1	34.4	117.5
M3(Y119A)	2.0	0.15	2.3	1.15	15.3
M3(Y119F)	2.1	0.16	27.1	12.9	169.4
M3(Y119A/N212F)	2.0	0.13	24.5	12.3	188.5
M3(Y119F/N212F)	0.16	0.10	122.0	763.0	1220.0
M3(Y119A/N212F/N213G)	2.4	0.11	17.7	7.4	161.0
M3(Y119F/N212F/ N213G)	0.08	0.13	52.3	653.0	402.0

[a] The average coefficient of variation was 15%. All point mutations are represented by their one-letter designations.

Table 3: Specific Activities of Recombinant Wild-Type, Chimeric, and Mutant Mu Class GSTs with the CDNBA Substrate

GST enzyme	specific activity [μmol min^{-1} (mg of protein)$^{-1}$]
M3-3	0.06 ± 0.02
M3-3(delPVC)	0.07 ± 0.02
M5-5	2.70 ± 0.30
$M3_{1-197}M5_{194-217}$	0.17 ± 0.04
$M5_{1-196}$ $M3_{201-224}$	0.12 ± 0.03
M3(N212F)	1.00 ± 0.25
M3(N212G)	0.07 ± 0.02
M3(N213G)	0.19 ± 0.03
M3(Y119A)	0.05 ± 0.02
M3(Y119F)	1.25 ± 0.20
M3(Y119A/N212F)	0.65 ± 0.07
M3(Y119F/N212F)	4.00 ± 0.30
M3(N212F/N213G)	0.90 ± 0.10
M3(N212G/N213G)	0.24 ± 0.06
M3(Y119A/N212F/N213G)	0.45 ± 0.07
M3(Y119F/N212F/N213G)	1.40 ± 0.20

(27.6 s^{-1}) and a lower K_m^{GSH} value (20 μM) compared to those of hGSTM3, but the K_m^{CDNB} value was unaffected. A single or double replacement of residues 212 and 213 with glycine (N212G and N213G) had only a moderate effect on the hGSTM3-3 activity (Table 2). Thus, the single N212F substitution produced an increase in k_{cat} and a decrease in K_m^{GSH} values, but the double replacement of N212F and N213G in hGSTM3-3 produced mainly increased turnover numbers (Table 2).

Tyr119 which is positioned near the active site pocket of the hGSTM3 subunit was replaced with alanine or phenylalanine. Surprisingly, the Y119A substitution had only a modest effect on catalysis of CDNB conjugation, slightly lowering the apparent k_{cat} value from 5.4 to 2.3 s^{-1}. In contrast, a Y119F substitution increased the k_{cat} value from 5.4 to 27 s^{-1} with K_m values similar to those of the Y119A mutant (Table 2).

Analyses of the Tyr119/Asn212 double substitutions were even more informative and revealed potential functions of these residues separately or together. The double mutant hGSTM3-3(Y119A/N212F) exhibited a k_{cat} value 5-fold greater than that of the wild-type enzyme and a k_{cat} value 10-fold greater than that of the hGSTM3-3(Y119A) single mutant, without affecting K_m values. The most notable effect, however, was observed with double mutant hGSTM3-3(Y119F/N212F); it was the most active of the chimeric enzymes with a k_{cat} value of 122 s^{-1} and a K_m^{CDNB} value

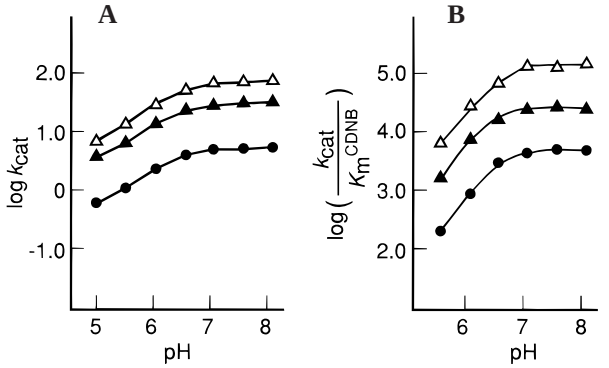

FIGURE 2: pH dependence of log k_{cat} (A) and log k_{cat}/K_m^{CDNB} (B). Data are for hGSTM3-3 (●), hGSTM3-3(N212F) (▲), and hGSTM3-3(N212F/N213G) (△), with CDNB as the substrate.

that was significantly lower (0.16 mM) than those (0.5−2.0 mM) of all other variants (Figure 1B and Table 2).

An additional N213G substitution introduced into the double mutants described above did not have a major impact on catalysis of the resultant triple mutants (Table 2). As a rule, the substitutions of Tyr119 with Ala or Phe and Asn212 with Phe mainly produced changes in apparent k_{cat} values and exhibited nearly additive effects with double (residues 119 and 212) replacements.

CDNBA is a much poorer substrate for hGSTM3-3 and hGSTM5-5 than is CDNB (Table 3), but the catalytic mechanism for this type of nucleophilic aromatic substitution reaction probably is not so different from that with CDNB. Catalysis with the CDNB substrate probably requires a relatively smaller free energy change from the ground state to a transition state compared with that of CDNBA, even though these two states probably do not overlap. Specific activities with the CDNBA substrate were also determined for different chimeric and mutant enzymes (Table 3). In this case, the hGSTM5-5 enzyme had an almost 50-fold greater activity than hGSTM3-3. In general, the specific activities of the hGSTM3,5-3,5 chimeric enzymes with CDNBA as a substrate paralleled their catalytic efficiencies with CDNB exhibiting activities intermediate between those of hGSTM3-3 and the more active hGSTM5-5 (Table 3). The hGSTM3-3 double mutant (Y119F/N212F) also had the highest specific activity with CDNBA (4 μmol min^{-1} mg^{-1}).

pH Dependence of Catalysis. The effect of pH on catalysis with CDNB as a substrate has been compared for wild-type

hGSTM3-3 and some of the chimeric enzymes (see Figure 2). There were no significant differences in the apparent pK_a values determined for wild-type hGSTM3-3 (6.5 ± 0.2) and those for mutant enzymes. The N212F mutation slightly lowered the apparent pK_a (6.2 ± 0.2), but the double mutation N212F/N213G did not affect the pH dependence of k_{cat}/K_m compared to that of the wild-type enzyme (pK_a = 6.6 ± 0.2). Other hGSTM3-3 mutants not shown in Figure 2 had very similar pH profiles and ionizations with apparent pK_a values that varied between 6.3 and 6.6; there was no evidence that the pH dependence of catalysis was substantially affected by any of the mutations described in this study.

Pre-Steady-State Kinetics. Rapid kinetics for wild-type hGSTM3-3 andh GSTM5-5 and mutant enzymes were analyzed by stopped-flow spectrophotometry. There was no evidence that the rate of product release is a rate-limiting step of catalysis. Even with protein concentrations as high as 10 or 20 μM, no burst increase of absorbance at 340 nm was detected in the first few milliseconds for any of the enzymes, including the hGSTM3-3(Y119F/N212F) mutant which has a low K_m^{CDNB} value (0.16 mM). Kinetic parameters calculated by linear regression analysis of the transient kinetics data were comparable to those obtained by steady-state analysis. Those results suggest that a chemical rather than physical step is rate-limiting in catalysis.

The hGSTM3-3 Active Site Structure. The crystal structure of the hGSTM3 subunit was recently determined as a catalytically active hGSTM2-3 heterodimer (Brookhaven PDB file 3GTU; Y. V. Patskovsky et al., manuscript in preparation). Although it has an overall fold very similar to those of the other mu class enzymes, the hGSTM3 subunit exhibits relatively high segmental flexibility, with poorly defined electron density of the C-terminal domain of the protein; thus, parts of the α4- and the N-terminal segment of the α5-helices (approximately between residues 110 and 130), in addition to the C-terminal peptide (residues 202−224), have increased motion relative to other mu class GSTs. The flexibility of part of the potential second substrate binding site (H-site) of hGSTM3-3 is consistent with its relatively low catalytic rate for nucleophilic aromatic substitution reactions (Tables 2 and 3).

In Figure 3, structures of hGSTM3 and hGSTM2 protein subunits are compared on the basis of corresponding G-sites. The main structural difference between the two GSTs is in the regions near their C-termini; this occurs as a consequence of multiple amino acid differences. Additionally, Pro206 is in a cis configuration in ligand-free hGSTM2 and hGSTM1a, whereas the homologous Pro210 of hGSTM3 is in a trans configuration. Although many of the amino acid substitutions of hGSTM3 relative to hGSTM2 and hGSTM1 are located in the C-terminal domain, certain structural features of the C-terminal segments of these enzymes are alike. For instance, the side chains at residues Asn212 and Asn213 are close to the active site pocket and their relative positions do not deviate significantly from those of Phe208 and Thr209 of hGSTM2 (see Figure 3A), or Phe208 and Ser209 of hGSTMla (data not shown). In general, the overall topology of the active site of hGSTM3 resembles that of other mu class proteins (panels A and B of Figure 3).

The three-dimensional structure of the GSH-binding G-site of hGSTM3 is virtually identical to those of other isoforms, because relative positions of side chains of residues involved in GSH binding are conserved. In that model of hGSTM3, the hydroxyl group of Tyr10 is about 3.5 Å from the sulfur atom of bound GSH. The ligand is anchored by at least 12 hydrogen bonds and electrostatic interactions between polar groups of GSH and the side chains at Tyr10, Trp11, Trp45, Arg46, Lys53, Asn62, Pro64, Gln75, and Ser76 of the same subunit, and Asp109 of the opposite subunit monomer. The rmsds between side chains atoms of these residues of hGSTM3 and their counterparts in hGSTM2 or hGSTM1a do not exceed 0.4 Å (except for that of Arg46). The potential catalytic site is formed by many additional residues, including Ile115, Leu16, Ile13, and Tyr119 (Figure 3C). For instance, Ile115 covers the most hydrophobic region of the pocket buried between the side chains of Ile13 and Leu114. The flexible Tyr119 ring is not farther than 4−4.5 Å from the Ile115 side chain, but the hydroxyl group is about 6−8 Å away from the sulfur atom of bound GSH (panels C and D of Figure 3). In addition, the two asparagine side chains (residues 212 and 213) are about 4.5−5.0 Å from the Tyr119 residue, and probably neither of them maintains hydrogen bond interaction with the hydroxyl group of Tyr119. The Asn212 residue is buried behind Tyr119, and its side chain protrudes deeply into a relatively hydrophobic pocket close to Ile115, Ile211, and Leu114 side chains (4.0−5.0 Å distances) (panels C and D of Figure 3). Hydrophobic contacts, including those between Ile13, Leu16, Ile115, Leu114, Tyr119, Ile211, and Trp218, are important in maintaining the enzyme tertiary structure and tie together domain I of the protein, the 4α-helix, and the C-terminal protein segments. Taken together, the structural information suggests that the presence of a polar Asn212 residue side chain should weaken these hydrophobic interactions and increase the segmental flexibility of hGSTM3 relative to that for other GSTs that have phenylalanine in that position.

DISCUSSION

The modular C-terminal domain interchange between hGSTM3 and hGSTM5 subunits and the point mutations introduced into the hGSTM3-3 enzyme identify regions of the protein that account for some of its unexpected catalytic properties. In particular, catalysis of nucleophilic aromatic substitution reactions is in large part influenced by the presence of a polar Asn212 residue in hGSTM3 instead of the hydrophobic phenylalanine residue found in that position for other mu class GSTs (Tables 2 and 3). Crystal structures suggest that the sequence divergence of the C-terminal domain of the hGSTM3 subunit could render this region generally more flexible than in the case of other GSTs. For the conjugation reaction of CDNB, residue 212 and the residue at position 119 (corresponding to residues 208 and 115 of other mu class GSTs) function in unison; for this reaction, replacement of both residues with phenylalanine (N212F and Y119F) converts a relatively ineffective hGSTM3-3 into a highly efficient enzyme (Figure 1B and Table 2).

Despite a relatively low degree of amino acid sequence identity (72%) between hGSTM3 and hGSTM5 subunits, three-dimensional structures of both homodimeric proteins are probably not so different from each other and from those of other mu class enzymes (panels A and B of Figure 3) especially at their putative GSH binding sites. Moreover, all mu class GSTs catalyze nucleophilic aromatic substitution

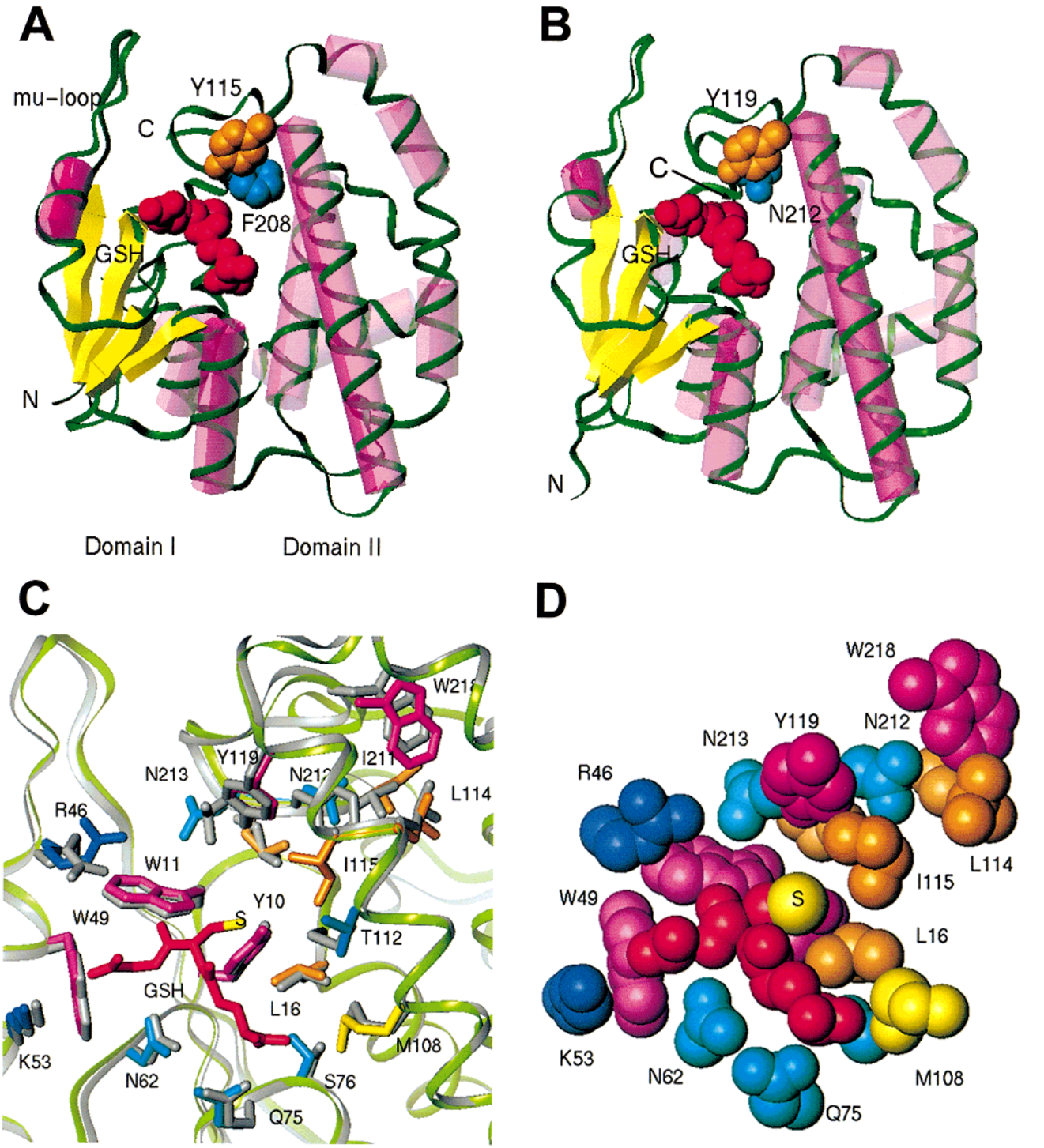

FIGURE 3: Structures of hGSTM3 and hGSTM2 subunits. The overall tertiary structures of the hGSTM2 subunit (PDB file 2GTU) (A) and the hGSTM3 subunit (3GTU) (B). Structural elements are α-helices shown as pink cylinders, *β*-sheets as yellow ribbons, and coils in green. Tyr115 (orange) and Phe208 (blue) side chains of the hGSTM2 subunit and the corresponding Tyr119 (orange) and Asn212 (blue) side chains of hGSTM3 are shown as CPK space-filling models. Bound GSH is red. The relative positions of the N- and C-termini of the proteins are represented by N and C, respectively, and structural domains I and II are assigned. (C) Alignment of hGSTM2 (gray) and hGSTM3 (different colors) active site structures. Atomic coordinates were determined on the basis of similarities between their G-site structures. Amino acid residues are labeled according to hGSTM3, and side chains of hGSTM3 are identified by the one-letter code. GSH is red with the sulfur atom in yellow. (D) Corresponding space-filling model of the side chains of the hGSTM3 active site structure. Hydrophilic amino acid side chains are dark and light-blue; hydrophobic residues are orange, and aromatic residues are pink. GSH is red. For viewing clarity, hydrogens and backbone atoms are not shown.

reactions with CDNB analogues with overlapping substrate specificities (*52*). The structural and biochemical similarities of these closely related isoenzymes provide a basis for engineering chimeric proteins that retain catalytic activities (Figure 1B and Tables 2 and 3). The hGSTM5 subunit has a much more hydrophobic C-terminus and is much more effective for CDNB conjugation than hGSTM3. Although significant differences exist between the primary structures of the hGSTM3 and hGSTM5 GST subunits, C-terminal domain interchange analysis suggests that their three-

dimensional structures are generally similar. Additional site-directed mutagenesis of hGSTM3-3 showed that the simple replacement of a polar amino acid residue, Asn2l2 of hGSTM3, with the corresponding phenylalanine residue found in most mu class enzymes produces a marked increase in catalytic efficiency of hGSTM3-3 with CDNB as the substrate. Kinetic analyses of different hGSTM3-3 mutants also demonstrated that ground and transition stabilization states for the reactions may be structurally different and distinct for the chimeric enzymes.

Similar biochemical properties of mu class GSTs, especially their ability to catalyze nucleophilic aromatic substitution reactions with CDNB as the substrate, suggest that CDNB binding and (or) CDNB catalytic sites for all of them are structurally and functionally similar. This inference predicts that within the same class of GST enzymes, amino acid residues from each can be substituted with corresponding residues from others without changing the overall protein fold or obliterating catalytic activity (see panels A and B of Figure 3). Reciprocal swapping of the most divergent C-termini of hGSTM3 and hGSTM5 subunits which share only 43% of their amino acid sequences does not abolish CDNB−GSH conjugation activity (Figure 1B). In addition, none of the mutations described here greatly affected apparent pK_a values of catalyzed reactions and binding of GSH (Figure 2). By contrast, some of the substitutions did have a marked influence on a chemical step of catalysis.

The hGSTM3-3 enzyme catalyzes many of the typical GST reactions (*45*), including CDNB−GSH conjugation, but does so with relatively low turnover numbers compared to that of other human mu class GSTs (except for hGSTM4-4; see ref *52*). The k_{cat}^{lim} value is about 10−20-fold lower than those of hGSTM1a-1a, hGSTM2-2, and hGSTM5-5. In contrast, the K_m^{CDNB} value is much greater, so the overall catalytic efficiency (k_{cat}/K_m^{CDNB} value) is about 100-fold lower than the values for most other mu class enzymes. Comparison of crystal structures of hGSTMla, hGSTM2, and hGSTM3 subunits demonstrates very similar α-backbone and most side chain atom conformations (*49*, *50*). Crystal structures for the hGSTM5 subunit are not yet available. Certain substitutions are located within the protein globules and often represent alternative variants such as Phe110 of hGSTM3 and Asn106 of hGSTM5, but most involve polar residues exposed to solvent. It is interesting that although a few variable residues are inside protein globules, at the intersubunit interface, or even close to active sites, there is usually sufficient three-dimensional volume to accommodate reciprocal replacements without changing the relative positions of atoms surrounding those residues or to bring about disruptions of the three-dimensional fold of the enzymes. For instance, in modeling analysis, Asn212 of hGSTM3 may be replaced with Phe or Tyr without affecting the protein conformation.

Asn212 of hGSTM3 that corresponds to Phe208 in other isoenzymes (Tyr208 of hGSTM4-4) is sandwiched between Tyr119 and Ile211 and lies close to the Ile115 side chain (panels C and D of Figure 3). The tertiary structure of the protein is stabilized in part by hydrophobic interactions between Leu114, Ile115, and Tyr119 of the α4-helix and the C-terminal domain Ile211 and Trp218 (panels C and D of Figure 3). The presence of the relatively polar Asn212 side chain in this hydrophobic crevice can weaken certain contacts and increase the mobility of protein segments that are close to the H-site. The fact that the structurally similar ligand-free forms of hGSTM2-2 and hGSTM1a-1a which have Phe208 in that position are much less flexible than hGSTM3-3 (*49*) corroborates such an idea. The relative rigidity of the C-terminus of ligand-free hGSTM2-2 in aqueous solution has also been recently confirmed by NMR studies (*53*).

Structural data do not provide any evidence that Asn2l2 is directly involved in catalysis. The Tyr119 and Asn213 side chains are in an intersubunit pocket between the two monomers of hGSTM3-3. The closest distances between Tyr119, Asn213, and the sulfur atom of bound GSH are about 6−8 Å. Because the dimensions of the planar second substrates (CDNB or CDNBA) are about 5−6 Å, the side chains of Tyr119 and Asn213 conceivably could be directly involved in substrate binding and/or transition-state stabilization. Indeed, it has been suggested that a corresponding Tyr115 residue of rat mu class enzymes functions in the chemical step of epoxide ring-opening reactions (*54*). However, replacement of the Asn213 side chain in the N213G substitution did not have a great effect on catalysis by the hGSTM3-3 mutants with the two substrates that were tested (Figure 1B and Tables 2 and 3). Thus, the Asn213 residue is probably sufficiently distant from the binding or transition-state site and does not significantly impact catalysis.

The N212F substitution in hGSTM3-3, however, greatly increased the catalytic efficiencies of the mutant enzymes compared to those that contain Asn212 (Table 2); this was accomplished mainly by an increase in k_{cat}^{lim} with a smaller effect on K_m^{CDNB}. Even the removal of the Asn212 side chain by the N212G substitution moderately increased catalytic efficiency values of mutants compared to those of wild-type hGSTM3-3. Therefore, kinetic and crystallographic data support a view that Asn212 is not directly involved in the GSH−CDNB conjugation reaction but rather has an important structural function; evidently, the nature of the side chain of residue 212 can govern the maintenance of the active site architecture of the enzyme.

Tyr119, which is close to the catalytic site, is one of a few amino acid residues that could be influenced by Asn212. Accordingly, Tyr119 was replaced with alanine or phenylalanine, and data for single mutants show that Tyr119 substitutions affected mainly k_{cat}^{lim} values that decreased in the following order: Ala119 < Tyr119 < Phe119 (Table 2). Apparently, Tyr119 of hGSTM3-3 and Asn212 are not directly involved in CDNB binding, but Asn212 may be responsible for the relatively slow rate of catalysis (for instance, transition-state stabilization) by this form of the enzyme. The presence of an amphipathic Tyr119 residue of wild-type hGSTM3-3 is probably not essential for catalysis because the Tyr119Ala substitution had little impact on steady-state kinetic constants. By contrast, the protein flexibility is probably greatly reduced after a Y119F substitution. It is also possible that the Y119F replacement changes the relative position of the newly introduced apolar phenylalanine side chain with respect to other residues. The Phe119 motion may thereby be restricted because of potential hydrophobic interactions with neighboring lle13, Leu16, and Ile115 side chains (panels C and D of Figure 3). However, this does not necessarily directly implicate Phe119 in

substrate binding, because an overall stabilization ("freezing") of protein tertiary or quaternary structure may increase the affinity for the substrate even if the binding sites are distant from Phe119. Accordingly, combined substitutions such as introducing a Phe119/Phe212 double mutation have a much greater influence on catalysis. The prominent increase in catalytic efficiency of a double phenylalanine mutant ($k_{cat}/K_m^{CDNB} = 7.6 \times 10^5\ s^{-1}\ M^{-1}$) also results from lowering of the K_m^{CDNB} value (0.16 mM). It is likely that the phenylalanine substitution at both positions effectively restricts the segmental mobility of these domains and provides for transition-state stabilization, thereby lowering the energy barrier for conversion of the enzyme−substrate complex into the product.

ACKNOWLEDGMENT

We thank Drs. Steven Almo and Alexander Federov for collecting and scaling the X-ray diffraction data, Drs. Sam Seifter and Vern Schramm for their valuable suggestions, and Dr. Michael Toney for his assistance in obtaining and interpreting the pre-steady-state kinetic data.

REFERENCES

1. Ketterer, B. (1988) *Mutat. Res. 202*, 343−361.
2. Jakoby, W. B., and Ziegler, D. M. (1990) *J. Biol. Chem. 265*, 20715−20718.
3. Tsuchida, S., and Sato, K. (1992) *Crit. Rev. Biochem. Mol. Biol. 27*, 337−384.
4. Rushmore, T. H., and Pickett, C. B. (1993) *J. Biol. Chem. 268*, 11475−11478.
5. Prestera, T., Zhang, Y., Spencer, S. R., Wilczak, C. A., and Talalay, P. (1993) *Adv. Enzyme Regul. 33*, 281−296.
6. Hayes, J. D., and Pulford, D. J. (1995) *Crit. Rev. Biochem. Mol. Biol. 30*, 445−600.
7. Gulick, A. M., and Fahl, W. E. (1995) *Pharmacol. Ther. 66*, 237−257.
8. Raha, A., and Tew, K. D. (1996) *Cancer Treat. Res. 87*, 83−122.
9. Wilkinson, J., and Clapper, M. L. (1997) *Proc. Soc. Exp. Biol. Med. 216*, 192−200.
10. Whalen, R., and Boyer, T. D. (1998) *Semin. Liver Dis. 18*, 345−358.
11. Mannervik, B., and Danielson, U. H. (1988) *CRC Crit. Rev. Biochem. 23*, 283−337.
12. Ketterer, B., and Christodoulides, L. G. (1994) *Adv. Pharmacol. 27*, 37−69.
13. Armstrong, R. N. (1994) *Adv. Enzymol. Relat. Areas Mol. Biol. 69*, 1−44.
14. Mantle, T. J. (1995) *Biochem. Soc. Trans. 23*, 423−425.
15. Van der Aar, E. M., Tan, K. T., Commandeur, J. N., and Vermeulen, N. P. (1998) *Drug Metab. Rev. 30*, 569−643.
16. Armstrong, R. N. (1998) *Curr. Opin. Chem. Biol. 2*, 618−623.
17. Ji, X., Zhang, P., Armstrong, R. N., and Gilliland, G. L. (1992) *Biochemistry 31*, 10169−10184.
18. Sinning, I., Kleywegt, G. J., Cowan, S. W., Reinemer, P., Dirr, H. W., Huber, R., Gilliland, G. L., Armstrong, R. N., Ji, X., and Board, P. G. (1993) *J. Mol. Biol. 232*, 192−212.
19. Dirr, H., Reinemer, P., and Huber, R. (1994) *Eur. J. Biochem. 220*, 645−661.
20. Wilce, M. C., and Parker, M. W. (1994) *Biochim. Biophys. Acta 1205*, 1−18.
21. Cameron, A. D., Sinning, I., L'Hermite, G., Olin, B., Board, P. G., Mannervik, B., and Jones, T. A. (1995) *Structure 3*, 717−727.
22. Armstrong, R. N. (1997) *Chem. Res. Toxicol. 10*, 2−18.
23. De Groot, M. J., and Vermeulen, N. P. (1997) *Drug Metab. Rev. 29*, 747−799.
24. Oakley, A. J., Bello, M. L., Battistoni, A., Ricci, G., Rossjohn, J., Villar, H. O., and Parker, M. W. (1997) *J. Mol. Biol. 274*, 84−100.
25. Prade, L., Huber, R., Manoharan, T. H., Fahl, W. E., and Reuter, W. (1997) *Structure 5*, 1287−1295.
26. Kamisaka, K., Listowsky, I., Gatmaitan, Z., and Arias, I. M. (1975) *Biochemistry 14*, 2175−2180.
27. Listowsky, I., Abramovitz, M., Homma, H., and Niitsu, Y. (1988) *Drug Metab. Rev. 19*, 305−318.
28. Listowsky, I. (1993) in *Hepatic Transport and Bile Secretion* (Tavolini, N., and Burk, P., Eds.) pp 397−405, Raven Press, New York.
29. Pickett, C. B., and Lu, A. Y. (1989) *Annu. Rev. Biochem. 58*, 743−764.
30. Board, P., Coggan, M., Johnston, P., Ross, V., Suzuki, T., and Webb, G. (1990) *Pharmacol. Ther. 48*, 357−369.
31. DeJong, J. L., Mohandas, T., and Tu, C. P. (1991) *Biochem. Biophys. Res. Commun. 180*, 15−22.
32. Daniel, V. (1993) *Crit. Rev. Biochem. Mol. Biol. 28*, 173−207.
33. Mannervik, B., Alin, P., Guthenberg, C., Jensson, H., Tahir, M. K., Warholm, M., and Jornvall, H. (1985) *Proc. Natl. Acad. Sci. U.S.A. 82*, 7202−7206.
34. Mannervik, B., Awasthi, Y. C., Board, P. G., Hayes, J. D., Di Ilio, C., Ketterer, B., Listowsky, I., Morgenstern, R., Muramatsu, M., and Pearson, W. R. (1992) *Biochem. J. 282*, 305−306.
35. Graminski, G. F., Kubo, Y., and Armstrong, R. N. (1989) *Biochemistry 28*, 3562−3568.
36. Liu, S., Zhang, P., Ji, X., Johnson, W. W., Gilliland, G. L., and Armstrong, R. N. (1992) *J. Biol. Chem. 267*, 4296−4299.
37. Dietze, E. C., Ibarra, C., Dabrowski, M. J., Bird, A., and Atkins, W. M. (1996) *Biochemistry 35*, 11938−11944.
38. Caccuri, M. A., LoBello, M., Nuccetelli, M., Nicotra, M., Rossi, P., Antonini, G., Federici, G., and Ricci, G. (1998) *Biochemistry 37*, 3028−3034.
39. Lai, H. C., Qian, B., Grove, G., and Tu, C. P. D. (1985) *J. Biol. Chem. 263*, 11389−11395.
40. Pearson, W. R., Vorachek, W. R., Xu, S. J., Berger, R., Hart, I., Vannais, D., and Patterson, D. (1993) *Am. J. Hum. Genet. 53*, 220−233.
41. Xu, S., Wang, Y., Roe, B., and Pearson, W. R. (1998) *J. Biol. Chem. 273*, 3517−3527.
42. Campbell, E., Takahashi, Y., Abramovitz, M., Peretz, M., and Listowsky, I. (1990) *J. Biol. Chem. 265*, 9188−9193.
43. Takahashi, Y., Campbell, E. A., Hirata, Y., Takayama, T., and Listowsky, I. (1993) *J. Biol. Chem. 268*, 8893−8898.
44. Patskovsky, Y., Huang, M. Q., Takayama, T., Listowsky, I., and Pearson, W. R. (1999) *Arch. Biochem. Biophys. 361*, 85−93.
45. Rowe, J. D., Patskovsky, Y. V., Patskovska, L. N., Novikova, E., and Listowsky, I. (1998) *J. Biol. Chem. 273*, 9593−9601.
46. Rowe, J. D., Tchaikovskaya, T., Shintani, N., and Listowsky I. (1998) *J. Androl. 19*, 558−567.
47. Rowe, J. D., Nieves, E., and Listowsky, I. (1997) *Biochem. J. 325*, 481−486.
48. Jensson, H., Alin, P., and Mannervik, B. (1985) *Methods Enzymol. 113*, 504−507.
49. Patskovsky, Y., Patskovska, L., and Listowsky I. (1999) *Biochemistry 38*, 1193−1202.
50. Patskovska, L. N., Fedorov, A. A., Patskovsky, Y. V., Almo, S. C., and Listowsky, I. (1998) *Acta Crystallogr. D 54*, 458−460.
51. Raghunathan, S., Chandross, R. J., Kretsinger, R. H., Allison, T. J., Penington, C. J., and Rule, G. S. (1994) *J. Mol. Biol. 238*, 815−832.
52. Comstock, K. E., Widersten, M., Hao, X. Y., Henner, W. D., and Mannervik, B. (1994) *Arch. Biochem. Biophys. 311*, 487−495.
53. McCallum, S. A., Hitchens, T. K., and Rule, G. S. (1999) *J. Mol. Biol. 285*, 2119−2132.
54. Johnson, W. W., Liu, S., Ji, X., Gilliland, G. L., and Armstrong, R. N. (1993) *J. Biol. Chem. 268*, 11508−11511.

BI991714T